

ed with an algorithm based on an optimally scaled template [P. Jonas, G. Major, B. Sakmann, *J. Physiol. (London)* **472**, 615 (1993)]; the threshold values were 0.8 ms for the 20 to 80% rise time and 25 to 50 pA for the peak amplitude. In the miniature IPSC experiments analyzed, the average frequency in control conditions was less than 2 Hz; superposition of independent miniature IPSCs by chance was thus unlikely. To quantify the contribution of GlyR- and GABA_A-mediated components in miniature IPSCs, we fit individual events with the function $f(t) = A_0 + A_1 I_{\text{GlyR}}(t) + A_2 I_{\text{GABAAR}}(t)$, where $I_{\text{GlyR}}(t)$ and $I_{\text{GABAAR}}(t)$ were average miniature IPSC templates obtained in the presence of bicuculline

and strychnine, respectively (baseline subtracted, peak amplitude normalized to 1). Variables A_1 and A_2 were obtained by multiple linear regression.

17. B. Katz, *The Release of Neural Transmitter Substances* (Liverpool Univ. Press, Liverpool, 1969); J. M. Bekkers and C. F. Stevens, *Nature* **341**, 230 (1989).

18. J. R. Mellor and A. D. Randall, *J. Physiol. (London)* **503**, 353 (1997).

19. P. M. Burger *et al.*, *Neuron* **7**, 287 (1991); C. Sagné *et al.*, *FEBS Lett.* **417**, 177 (1997).

20. J. M. Juiz, R. H. Helfert, J. M. Bonneau, R. J. Wenthold, R. A. Altschuler, *J. Comp. Neurol.* **373**, 11 (1996).

21. J. C. Eccles, *The Physiology of Synapses* (Springer-Verlag, Berlin, 1964).

22. J. Tegnér, T. Matsushima, A. El Manira, S. Grillner, *J. Neurophysiol.* **69**, 647 (1993).

23. W. Brune *et al.*, *Am. J. Hum. Genet.* **58**, 989 (1996).

24. We thank J. R. P. Geiger, M. V. Jones, M. Martina, and K. Starke for critically reading the manuscript, and B. Sakmann for helpful discussions. We also thank B. Hillers for secretarial assistance, S. Pfützinger for construction of equipment, and Novartis for providing baclofen. Supported by the DFG (grant Jo-248/2-1 and Sa-435/10-2).

30 March 1998; accepted 9 June 1998

Spatial Organization of Transcription Elongation Complex in *Escherichia coli*

Evgeny Nudler,* Ivan Gusarov, Ekaterina Avetissova, Maxim Kozlov, Alex Goldfarb

During RNA synthesis in the ternary elongation complex, RNA polymerase enzyme holds nucleic acids in three contiguous sites: the double-stranded DNA-binding site (DBS) ahead of the transcription bubble, the RNA-DNA heteroduplex-binding site (HBS), and the RNA-binding site (RBS) upstream of HBS. Photochemical cross-linking allowed mapping of the DNA and RNA contacts to specific positions on the amino acid sequence. Unexpectedly, the same protein regions were found to participate in both DBS and RBS. Thus, DNA entry and RNA exit occur close together in the RNA polymerase molecule, suggesting that the three sites constitute a single unit. The results explain how RNA in the integrated unit RBS–HBS–DBS may stabilize the ternary complex, whereas a hairpin in RNA result in its dissociation.

The paradox of transcription elongation is the ability of RNA and DNA to pass through RNA polymerase (RNAP) within an extremely stable ternary complex. To explain protein–DNA–RNA interaction that is both tight and flexible, investigators have proposed the concept of the sliding clamp (1, 2) by analogy with the DNA replication apparatus (3).

In our current thinking, the sliding clamp consists of three putative elements (Fig. 1). DBS, which is defined as the region of strong nonionic interaction between RNAP and the template, has been mapped to ~9 base pairs (bp) of DNA duplex just ahead of the point where DNA forks out into the transcription bubble (2). Recently, we presented evidence that the template DNA strand in the bubble forms an ~8-bp hybrid (4), which is held in RNAP by weak ionic interactions (2) that define HBS. The notion of a distinct site holding single-stranded RNA leading out of the active center (RBS), first proposed two

decades ago (5), has been extensively discussed recently (6). Together, HBS and RBS should cover 14 to 16 3'-proximal nucleotides of RNA, in accord with ribonuclease protection data (5, 7, 8). The observation that the RNA secondary structure (hairpins) at 7 to 9 nucleotides from the 3' terminus destabilizes the ternary elongation complex (TEC) (9) indicates that this may be the area of crucial protein–RNA interactions. Here we directly identify RNA, DNA, and protein segments involved in close contacts. The results show that RBS, HBS, and DBS are integrated in the RNAP molecule, which has important implications for the mechanism of RNA chain elongation and termination.

To map RNA-protein contacts along the trajectory of RNA, we used a photoreactive analog of uridine, 4-thio-uridine (Fig. 2A), incorporated into a single position of RNA transcript. The probe has a reagent arm less than 1 Å long and passes unimpeded through the protein as the complex advances (Fig. 2B). We induced cross-linking by ultraviolet (UV) irradiation of TEC that has been stalled at defined positions. The probe was incorporated at either position +21 or +45 relative to the RNA 5' terminus (Fig. 2B, lanes 2 to 14 and 15 to 18, respectively).

Judging from the relative yield of cross-

linking with the +21 probe, close RNA contacts with RNAP β' subunit, and to a lesser extent with the β subunit, occur near the active site (position -1 relative to the 3' terminus). The segment of at least four nucleotides from -3 to -6 appears not to be involved in close β', β contacts. Further upstream, the close contacts (β' >> β) occur within the nine-nucleotide segment from -10 to -18. Because of the sequence constraints, contacts at -7 to -9 could not be scanned with the +21 probe. However, with the +45 probe (lanes 15 to 18), RNA nucleotide at -8 displays a cross-linking yield of intermediate intensity, suggesting that it is on the borderline of the close RNA-protein contact area. In the case of the +45 probe, two β'-cross-linked species could be resolved (lanes 17 and 18) because of the longer RNA moiety.

Qualitatively similar results were obtained when the azido-uridine probe with longer (~8 Å) reagent arm was used (Fig. 2A), but the difference between cross-linking of different transcript segments was less pronounced (8).

For unambiguous interpretation of the results, it was essential to establish that the stalled TECs used for cross-linking were not backtracked (4, 7) (Fig. 2C). To this end, a control experiment was performed in which backtracking in TEC56 (cross-linking probe at -12) was either induced or suppressed by incorporating helix-destabilizing (inosin) or stabilizing [5-bromo-uridine triphosphate (5-bromo-UTP) and 5-iodo-cytosine triphosphate (5-iodo-CTP)] nucleotides, respectively, into the 3' proximal region of the transcript (4). The backtracked complex was identified by its failure to elongate RNA (Fig. 2C, bottom panel, lane 4) and by its sensitivity to transcript cleavage factor GreB (lane 5). Evidently, prominent RNA-protein cross-linking occurred only in the productive complex, not in the backtracked complex (Fig. 2C, top panel). In addition, antisense oligonucleotides known to inhibit backtracking (7) had no effect on the cross-linking results obtained with TEC30, TEC34, and TEC38 (8).

To map the cross-linking sites, we excised from the gel of Fig. 2B the species of β or β' cross-linked to RNA. The analysis was performed for TECs with the probe positioned at +21 (TEC30, TEC34, TEC38, TEC43, and

E. Nudler and I. Gusarov, Department of Biochemistry, New York University Medical Center, New York, NY 10016, USA. E. Avetissova, M. Kozlov, A. Goldfarb, Public Health Research Institute, New York, NY 10016, USA.

*To whom correspondence should be addressed. E-mail: evgeny.nudler@med.nyu.edu

REPORTS

TEC53) and at +45 (TEC52**) relative to the 5' terminus, thus scanning crosslinks at -10, -14, -18, -23, -33, and -8, respectively from the 3' terminus (Fig. 3). The

excised radioactive species were subjected to limited chemical degradation at Met or Cys residues under single-hit conditions, that is, when less than one cleavage occurred per

polypeptide chain. This procedure yields a mixture of two families of nested polypeptides representing the COOH- and NH₂-termini of the subunit. Degradation products were resolved by SDS-polyacrylamide gel electrophoresis (SDS-PAGE) under conditions favoring resolution of small fragments.

In the β' subunit, short Cys fragments can originate only from the NH₂-terminus (Fig. 3C). Hence, the characteristic cluster of fragments 58, 70, 72, 85, and 88 in the case of TEC34 and TEC38 (Fig. 3B) indicates that there is a strong RNA-protein crosslink within the first 58 residues of β' (heavy arrow in Fig. 3C). This conclusion is reinforced by the NH₂-terminus-specific cluster of Met fragments 102, 130, and 151 in the case of TEC34 and TEC38 (Fig. 3A). The appearance of Met fragment 29 in the case of TEC43 suggests another NH₂-terminal crosslinking site within the first 29 residues of β' (dotted arrow in Fig. 3C).

The NH₂-terminal crosslinks found in TEC34, TEC38, and TEC43 are absent in TEC30 because the shortest Cys and Met fragments seen are 366 and 330, respectively, which point to a more distal crosslink (gray arrow in Fig. 3C). However, when the short-armed 4-thio-uridine monophosphate (UMP) probe in TEC30 is replaced by the longer-armed "azido"-UMP in TEC30*, cross-linking in the NH₂-terminus does take place, as can be seen from the reappearance of the NH₂-terminus-specific clusters of Met and Cys fragments. In TEC53, in which the probe has moved 33 nucleotides away from the 3' terminus, no NH₂- (or COOH-) terminal crosslinks were detected (Fig. 3).

As noted above, in the case of TEC52** carrying the longer transcript cross-linked through the -8 position, two cross-linked spe-

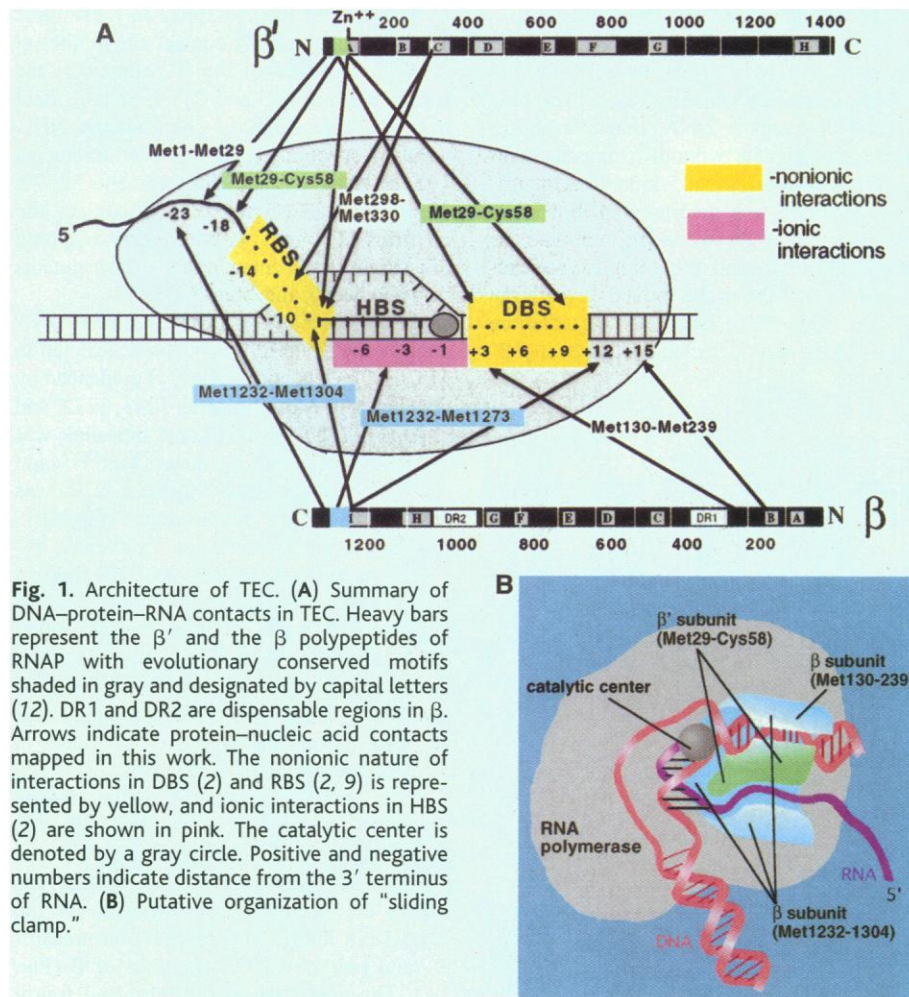
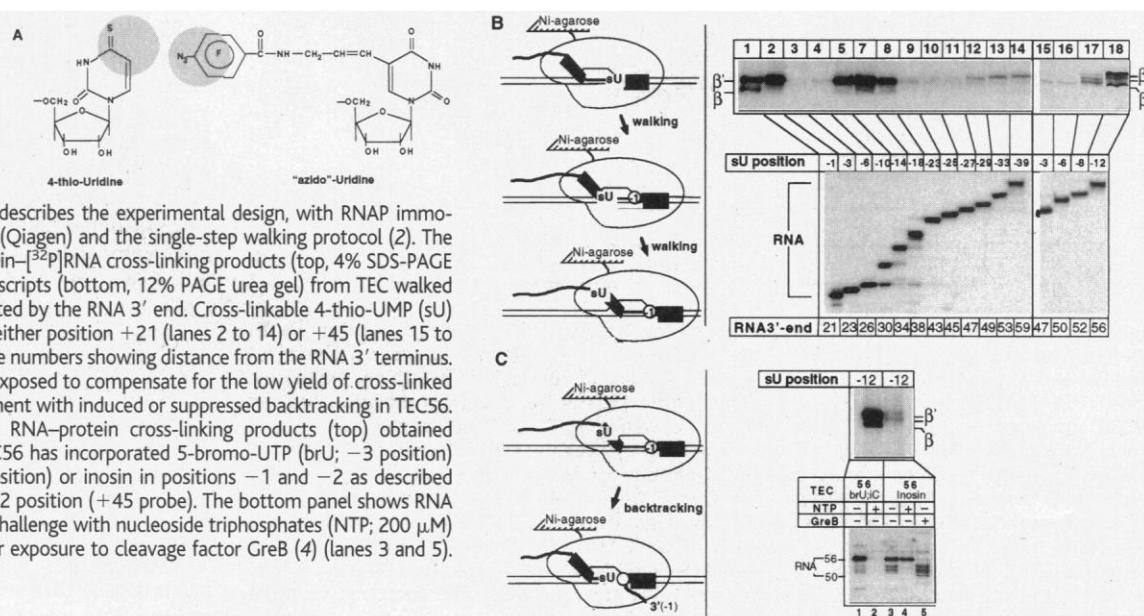


Fig. 1. Architecture of TEC. (A) Summary of DNA-protein-RNA contacts in TEC. Heavy bars represent the β' and the β polypeptides of RNAP with evolutionary conserved motifs shaded in gray and designated by capital letters (72). DR1 and DR2 are dispensable regions in β. Arrows indicate protein-nucleic acid contacts mapped in this work. The nonionic nature of interactions in DBS (2) and RBS (2, 9) is represented by yellow, and ionic interactions in HBS (2) are shown in pink. The catalytic center is denoted by a gray circle. Positive and negative numbers indicate distance from the 3' terminus of RNA. **(B)** Putative organization of "sliding clamp."

Fig. 2. RNA-protein cross-linking in TEC. (A)

Photoreactive cross-linkable nucleotide derivatives used as cross-linking probes (75). Reactive groups are encircled. **(B)** The principal experiment. Scheme on the left describes the experimental design, with RNAP immobilized on Ni-agarose resin (Qiagen) and the single-step walking protocol (2). The autoradiogram shows protein-[³²P]RNA cross-linking products (top, 4% SDS-PAGE gel) and free [³²P]RNA transcripts (bottom, 12% PAGE urea gel) from TEC walked (76) to the positions indicated by the RNA 3' end. Cross-linkable 4-thio-UMP (sU) probe was incorporated in either position +21 (lanes 2 to 14) or +45 (lanes 15 to 18), as indicated by negative numbers showing distance from the RNA 3' terminus. The bottom gel was underexposed to compensate for the low yield of cross-linked species. **(C)** Control experiment with induced or suppressed backtracking in TEC56. The autoradiogram shows RNA-protein cross-linking products (top) obtained under conditions when TEC56 has incorporated 5-bromo-UTP (brU; -3 position) and 5-iodo-CTP (iC; -4 position) or inosin in positions -1 and -2 as described (4). 4-Thio-UMP was at -12 position (+45 probe). The bottom panel shows RNA transcripts before or after challenge with nucleoside triphosphates (NTP; 200 μM) for 2 min (lanes 2 and 4) or exposure to cleavage factor GreB (4) (lanes 3 and 5).



REPORTS

cies of β' were recovered (Fig. 2B, lane 17). Mapping of the crosslink in the fast moving (bottom) species revealed the NH_2 -terminal contact evident from the appearance of the Met^{102} and Cys^{58} fragments (Fig. 3). Upon degradation, however, the top species crosslink yielded only the Met^{330} and Cys^{366} fragments, which are characteristic of the more distal crosslink (gray arrow in Fig. 3C).

From these data, we conclude that, in TEC, the NH_2 -terminus of the β' subunit is involved in the contacts with RNA in the putative RBS upstream from position -8 relative to the transcript 3' terminus.

A similar analysis of RNA crosslinks in the β subunit revealed contacts near the COOH-terminus (Fig. 4). These contacts are evident from the appearance of the COOH-terminal-

specific cluster of Met fragments 1243, 1232, and 1230 in the cases of TEC30, TEC34, and TEC52**, representing the -10 , -14 , and -8 probes respectively. In TEC38 (-18 probe), a more distal crosslink was revealed by the cluster of Met fragments 1304, 1290, and 1273.

To map DNA-protein contacts in TEC, we took advantage of the end-to-end template-switching reaction whereby RNAP, reaching the end of template DNA, transfers onto a secondary template without losing the transcript (2). Photoreactive 5-iodo-2'-deoxyuridine (Fig. 5A) was incorporated into a defined position of the secondary template (its template strand), and the complex was advanced so that the probe moved through the protein (Fig. 5C). Upon UV irradiation, cross-linking was detected in the β and β'

subunit. Cross-linking to the β' subunit was predominant in the putative DBS region encompassing ~ 9 bp of double-stranded DNA ahead of the bubble (2), that is, in TEC67, TEC64, and TEC61 (Fig. 5C).

Mapping of the crosslinks in these three TECs revealed a DNA contact site or sites at the NH_2 -terminus of the β' subunit in the area between Met^{29} and Cys^{58} , as is evident from the appearance of characteristic NH_2 -terminal-specific clusters of Met fragments 102, 130, and 151 and Cys fragments 58, 70, 72, 85, and 88 (Fig. 5D). This contact site confirms our previous preliminary mapping of a single DBS contact point to the segments between Met^{29} and Met^{102} (2).

In the β subunit, a COOH-terminal DNA contact site distal to Met^{1243} was detected in TEC67, TEC64, and TEC61, as evidenced by the cluster of Met fragments 1243, 1232, and 1230 (Fig. 5E). An additional crosslink was deduced between residues Met^{130} and Met^{239} , because Met fragment 239 was prominent in the β subunit digest (Fig. 5E).

The principal conclusion from these results is that DNA contacts in DBS involve both the NH_2 -terminus of β' and the COOH-terminal of β , that is, the same regions as the RNA contacts in RBS (Fig. 1A). Of course, these are not the only protein-nucleic acid contacts, as indicated by overlapping patterns of NH_2 - and COOH-terminal fragments in some of the degradation reactions.

These results establish a spatial linkage between four structural elements of TEC: (i) the ~ 9 -bp DNA duplex ahead of the bubble, (ii) the ~ 8 -nucleotide RNA segment upstream of the distal (-8) position of the RNA-DNA hybrid, (iii) the NH_2 -terminus of β' , and (iv) the COOH-terminus of β (Fig. 1A). The proximity of the third and fourth elements agrees with the recent report that β and β' can be genetically fused without loss of RNAP function (10).

We propose a model of TEC in which these four elements are integrated into a single unit (integrated DBS-RBS, or "double sliding clamp"), thereby serving the conflicting requirements of elongation: strong binding combined with smooth sliding (Fig. 1B). One side of this unit contains the openings for DNA entry and for RNA exit. The other side is linked to the active center and adjacent DNA-RNA hybrid. The incomplete helix turn resulting from the ~ 8 -bp hybrid (4) and DNA bending (11) ensures that the trajectory of outgoing RNA is antiparallel with the incoming DNA. The evolution conservation of elements iii and iv (12) and similar biochemical properties of eukaryotic and prokaryotic TECs (6) suggest that the proposed model could be of a general nature.

In our previous work, we showed that DNA interactions in DBS are essential for stable salt-resistant RNA interactions in RBS (2) and vice

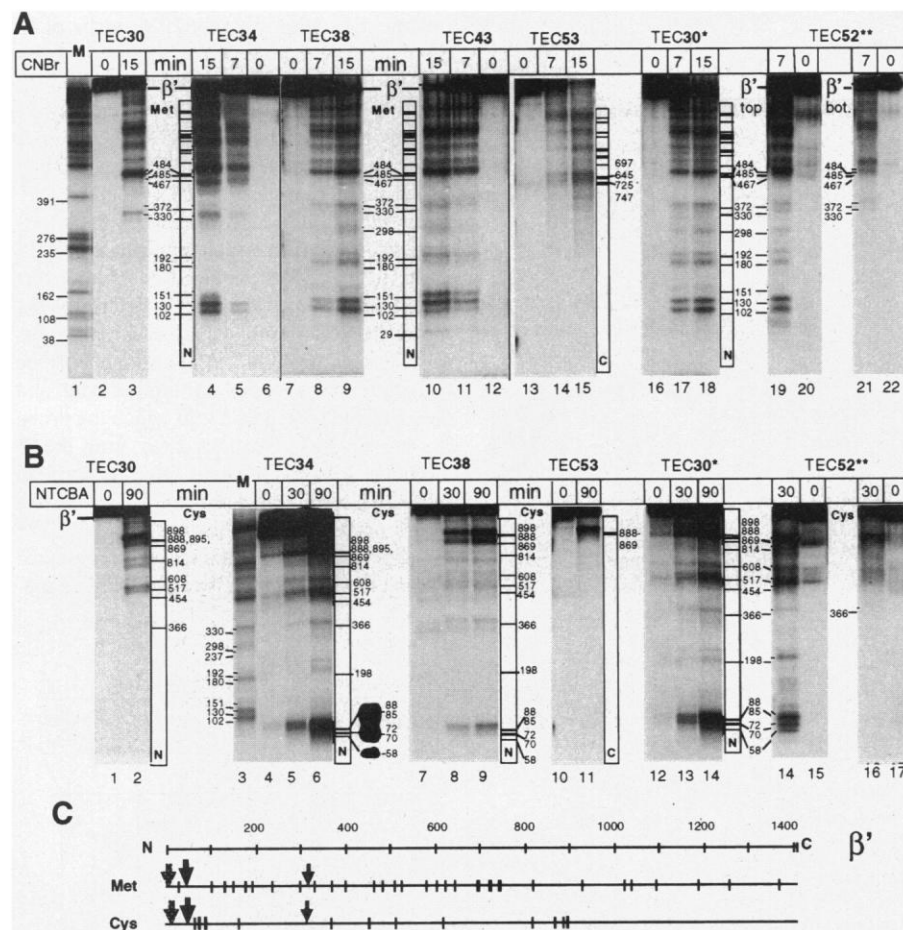


Fig. 3. Mapping of RNA crosslinks in the β' subunit by single-hit cleavage at Met (A) and Cys (B) residues. Autoradiograms of gradient (7 to 14%; 20 cm) SDS-PAGE gels show products of time-dependent partial degradation with cyanogen bromide (CNBr) or 2-nitro-5-thiocyanobenzoic acid (NTCBA) (14) of the cross-linked β' material from TECs of Fig. 2 or from similarly obtained TEC30* carrying the long-armed "azido"-UMP derivative (Fig. 1). TEC52** carries the +45 reactive probe. The insert (B, lane 6) shows the shortest labeled Cys fragments resolved on 46 cm of 8.5% SDS-PAGE gel. Bar columns present theoretical patterns of the NH_2 -terminal (N) and COOH-terminal (C) families of Met and Cys fragments, with the numbers indicating residue positions in the β' polypeptide. As the reference marker, CNBr degradation products of the β subunit labeled near Met^{1304} are shown in lane M (A) and β' subunit labeled near Met^{102} (B). (C) Chemical degradation map of the β' subunit. Horizontal lines symbolize 1407-amino acid β' polypeptide. Vertical lines represent distributions of Met and Cys cleavage sites. The locations of three cross-linking sites are indicated by three different arrows.

REPORTS

versa (13); to explain this, we suggested an allosteric model of RBS-DBS communication (2). The integrated DBS-RBS model presented here implies that the functional link between DBS and RBS may be direct rather than allosteric. In other words, the RNA segment upstream of the hybrid may constitute a structural element of the DNA clamp. This explains how an RNA hairpin formed eight nucleotides upstream of the RNA 3' terminus would destabilize TEC (9); It would literally unlock the double-sliding clamp and thereby open the way to termination.

References and Notes

1. S. A. Darst, E. W. Kubalek, R. D. Kornberg, *Nature* **340**, 730 (1989); A. Polyakov, E. Severinova, S. A. Darst, *Cell* **83**, 365 (1995).
2. E. Nudler et al., *Science* **273**, 211 (1996).
3. J. Kurijan and M. O'Donnell, *J. Mol. Biol.* **234**, 915 (1994).
4. E. Nudler et al., *Cell* **89**, 33 (1997).
5. S. A. Kumar and J. S. Krakow, *J. Biol. Chem.* **250**, 2878 (1975).
6. S. M. Uptain et al., *Annu. Rev. Biochem.* **66**, 117 (1997).

Fig. 4. Mapping of RNA crosslinks in the β subunit by single-hit cleavage at Met residues (A). Scheme of distribution of Met cleavage sites along 1342-amino acid β polypeptide is shown at the bottom (B), with the two crosslinks indicated by arrows.

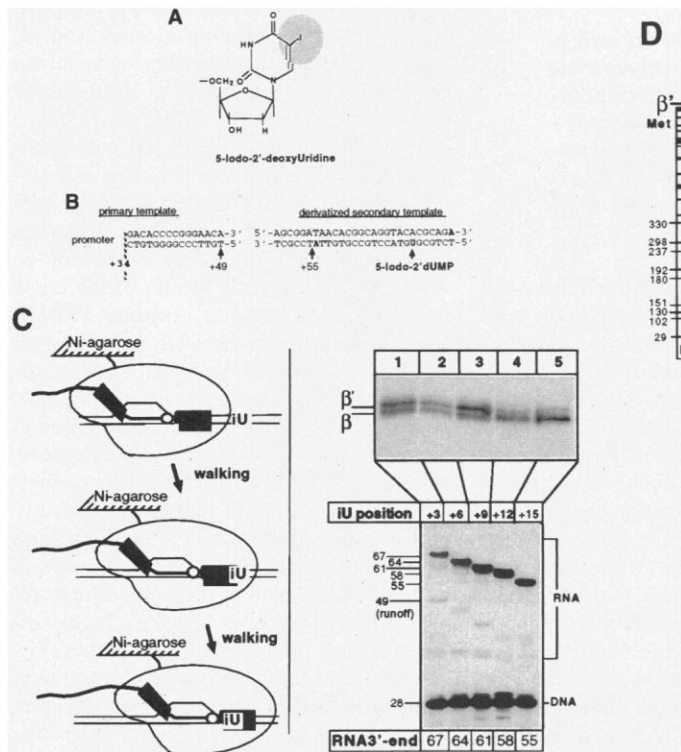
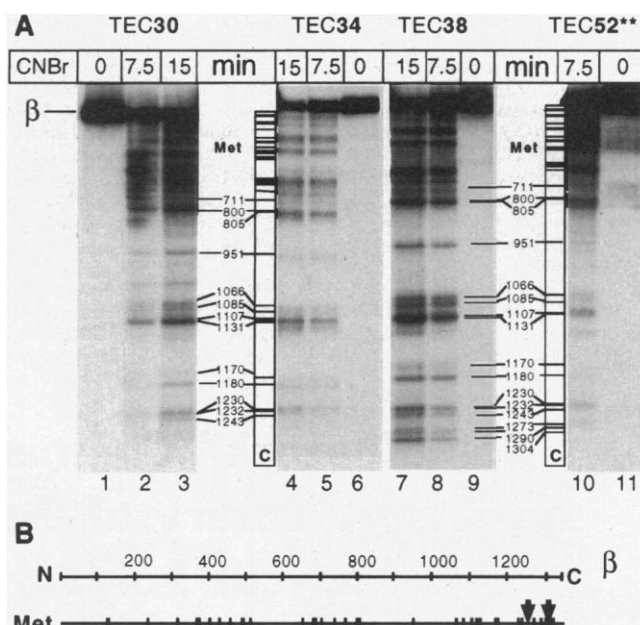
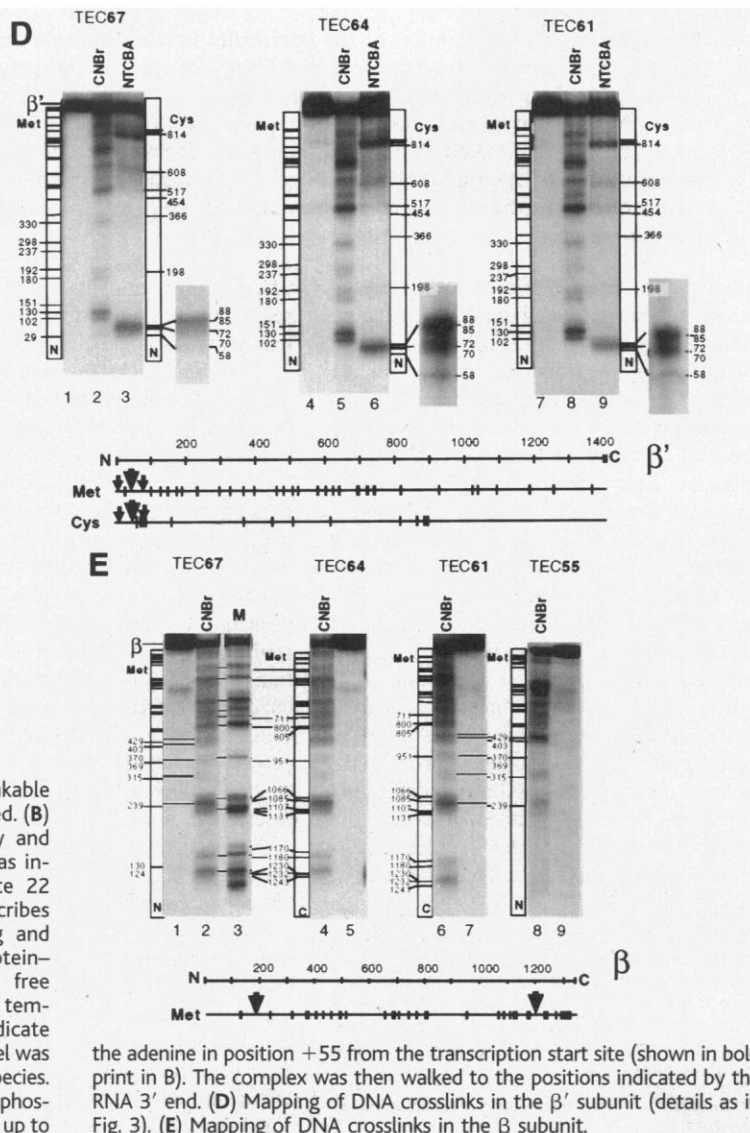


Fig. 5. DNA-protein cross-linking in TEC. (A) Photoreactive cross-linkable nucleotide used as cross-linking probe; the reactive group is encircled. (B) Structure and sequence of the relevant sections of the primary and secondary templates. The probe [15-iodo-2'-deoxyuridine (iU)] was incorporated into the template strand of the secondary template 22 nucleotides downstream from its 3' end (15). (C) The scheme describes the experimental design based on the combination of walking and template-switching protocols (2). The autoradiogram shows protein- ^{32}P DNA cross-linking products (top, 4% SDS-PAGE gel) and free ^{32}P RNA transcripts, together with end-labeled secondary DNA template fragment (bottom, 12% PAGE urea gel). Positive numbers indicate the distance of the iU probe from the RNA 3' terminus. The bottom gel was underexposed to compensate for the low yield of cross-linked species. Prelabeled TEC switched templates (2) in the absence of adenosine triphosphate to ensure unidirectional transcription of the secondary template up to



the adenine in position +55 from the transcription start site (shown in bold print in B). The complex was then walked to the positions indicated by the RNA 3' end. (D) Mapping of DNA crosslinks in the β ' subunit (details as in Fig. 3). (E) Mapping of DNA crosslinks in the β subunit.

7. N. Komissarova and M. Kashlev, *J. Biol. Chem.* **272**, 15329 (1997).
8. E. Nudler *et al.*, unpublished results.
9. K. M. Arndt and M. J. Chamberlin, *J. Mol. Biol.* **213**, 79 (1990); K. S. Wilson and P. H. von Hippel, *Proc. Natl. Acad. Sci. U.S.A.* **92**, 8793 (1995); E. Nudler *et al.*, *Cell* **81**, 351 (1995).
10. K. Severinov *et al.*, *J. Biol. Chem.* **272**, 24137 (1997).
11. W. A. Rees *et al.*, *Science* **260**, 1646 (1993).
12. G. Puhler *et al.*, *Proc. Natl. Acad. Sci. U.S.A.* **86**, 4569 (1989); D. Sweetser, M. Nonet, R. A. Young, *ibid.*, **84**, 1192 (1987).
13. S. Borukhov *et al.*, *J. Biol. Chem.* **268**, 23477 (1993); K. Severinov and A. Goldfarb, *ibid.*, **269**, 31701 (1994).
14. V. Markovtsov *et al.*, *Proc. Natl. Acad. Sci. U.S.A.* **93**, 3221 (1996).
15. "Azido"-UTP is 5-(*p*-azidotetrafluoro)benzamido-alil-uridine triphosphate. The complete synthesis of "azido"-UTP will be published elsewhere. 4-thio-UTP was synthesized from 4-thio-UMP (Sigma) as described (14). 5-Iodo-2'-deoxyuridine containing DNA oligonucleotide was custom synthesized (Oligos Etc., Wilsonville, OR).
16. Walking reactions were as described (2), except that several positions (+12, +15, +17, +39, +40, +41, +42) in the transcript were radiolabeled with [³²P]cytosine monophosphate and [³²P]guanosine monophosphate, the cross-linking with 4-thio-UMP was induced by UV irradiation at 365 nm as in (14), the cross-linking with "azido"-UMP was induced by UV irradiation at 308 nm for 5 min, and the cross-linking with 5-iodo-2'-deoxyuridine was performed

as in (2). The template used was the T7A1 promoter fragment (153-pb), obtained by polymerase chain reaction with the following transcribed sequence: ATCGAGAGGGACACGCGAATAGCCATCCCAATCGAACAGGCTGCTGGTAATCGCAGGCTGGAGACTTGGATCCCCGGGTA.

17. We are grateful to O. Bereschenko for help with the figures, A. Mustaev for advice on cross-linking techniques, and Sergei Borukhov for GreB. This work was supported by NIH grant GM49242 (A.G.) and departmental funds (E.N.). E.A. and M.K. are in the graduate programs of the Institute of Molecular Genetics, Russian Academy of Sciences, and the Linnological Institute (Irkutsk, Russia), respectively.

6 January 1998; accepted 8 June 1998

Combinatorial Chemistry in Insects: A Library of Defensive Macrocylic Polyamines

Frank C. Schröder,* Jay J. Farmer, Athula B. Attygalle, Scott R. Smedley, Thomas Eisner, Jerrold Meinwald

The pupal defensive secretion of the coccinellid beetle *Epilachna borealis* is composed principally of a combinatorial library of macrocylic polyamines. These compounds constitute a previously unrecognized family of natural products, characterized by extremely large-ring lactonic structures derived from a small set of (2-hydroxyethylamino)alkanoic acids. The combinatorial assembly of these simple building blocks generates a high degree of structural diversity, which is further increased by slow, spontaneous intramolecular rearrangement of the macrocycles.

Insect pupae, given that they cannot crawl, run, or fly, should be vulnerable to predation. However, many benefit from concealment and camouflage or from mechanical means of defense (1), and there are a few documented cases of pupae that are protected chemically. Pupae of coccinellid beetles (2) of the genus *Epilachna* bear a dense coating of glandular hairs that secrete oily droplets deterrent to insects (Fig. 1) (3, 4). In *E. varivestis* (the Mexican bean beetle), the active principles of this secretion are azamacrolides, novel lactones with a single nitrogen atom incorporated into a ring of 13 to 16 members (Fig. 1, compound 1) (4). Gas chromatographic analyses of the pupal secretion of the squash beetle, *E. borealis*, have indicated only the presence of vitamin E acetate and other tocopherol derivatives (4, 5). However, in tests with ants, these compounds proved to be essentially inactive, whereas the secretion itself was potentially deterrent. To find and iden-

tify the active components in the *E. borealis* secretion, we therefore adopted a more general analytical approach.

Any analytical method with an initial chromatographic separation is likely to discriminate against some classes of components and to favor others. In studying a biological extract of mostly unknown composition, therefore, it is expedient to begin with a direct nuclear magnetic resonance (NMR) spectroscopic investigation of the total, unfractionated natural sample. Following this principle, we carried out NMR spectroscopic studies of freshly obtained *E. borealis* secretion (6). One- and two-dimensional ¹H NMR experiments revealed that the tocopheryl acetates account for only a relatively small percentage of the beetles' total secretion (~20%), whereas the major components represented a group of previously undetected compounds. By analysis of (¹H,¹H) exclusive correlation spectroscopy (7), (¹³C,¹H) gradient-enhanced heteronuclear single-quantum coherence (8), and (¹³C,¹H) gradient-enhanced heteronuclear multiple bond correlation spectra of the mixture, these components were shown to be esters and amides derived from the carboxyl- and the 2-hydroxyethylamino moieties of several (ω-1)-(2-hydroxyethylamino)alkanoic acids. To determine the chain lengths of these acids, we carried out an

alkaline hydrolysis of the crude secretion, followed by methylation with diazomethane and trifluoroacetylation with trifluoroacetic acid anhydride. This procedure afforded a mixture of N,O-bis-trifluoroacetylated methyl esters of three homologous (ω-1)-(2-hydroxyethylamino)alkanoic acids, 2 to 4, which could be analyzed by gas chromatography-mass spectrometry (GC-MS) (9). The major component (~90%) of the alkaline hydrolysate, 10-(2-hydroxyethylamino)undecanoic acid (4) was isolated by column chromatography and characterized by its ¹H and ¹³C NMR spectra (10).

Whether the newly detected components are simply intramolecular lactones and lactams, that is, azamacrolides or their lactam isomers, or whether they each incorporate more than one acid moiety could not be determined from NMR spectra of the crude mixture alone. However, because GC-MS analysis of the crude secretion did not reveal any volatile components other than the already described tocopheryl acetates, the new *E. borealis* secretion components appeared to be higher molecular weight cyclic oligomers combining several (ω-1)-(2-hydroxyethylamino)alkanoic acid (2 to 4) units. This hypothesis was corroborated by high-pressure liquid chromatography (HPLC) analyses with a mass spectrometric detector, which revealed the secretion to contain a highly diverse mixture of macrocylic polyamines (Fig. 2) (11). The major components are series of homologous trimers, tetramers, and pentamers of the three acids 2 to 4, along with smaller quantities of dimers, hexamers, and heptamers (12). Furthermore, the secretion contains several isomers of each oligomer. Using repeated preparative HPLC fractionation, we isolated the most abundant trimeric, tetrameric, and pentameric components of the earliest eluting (Fig. 2) series of compounds (13). One- and two-dimensional ¹H NMR spectroscopic analyses (14) showed these components to be the symmetric macrocylic lactones 6, 7, and 8 derived from three, four, or five units, respectively, of 10-(2-hydroxyethylamino)undecanoic acid (4) (Fig. 1). Thus, the earliest eluting, most abundant isomers of the oligomers appear to repre-

F. C. Schröder, J. J. Farmer, A. B. Attygalle, J. Meinwald, Baker Laboratory, Department of Chemistry, Cornell University, Ithaca, NY 14853, USA. S. R. Smedley, Department of Biology, Trinity College, Hartford, CT 06106, USA. T. Eisner, Section of Neurobiology and Behavior, Seeley G. Mudd Hall, Cornell University, Ithaca, NY 14853, USA.

*To whom correspondence should be addressed. E-mail: fs31@cornell.edu